Journal of Oceanology and Limnology
Vol. 39 No. 1, P. 340-349, 2021
https://doi.org/10.1007/s00343-020-0117-3

UPLC-MS metabolomics provides insights into the differences between black- and white-shelled Pacific oysters *Crassostrea gigas**

Xi CHEN, Qiuyun JIANG, Hongce SONG, Lingling LI, Chaoyi XIE, Baoyu HUANG, Yaqiong LIU, Meiwei ZHANG, Lei WEI**, Xiaotong WANG**

School of Agriculture, *Ludong University*, *Yantai 264025*, *China*

Received Mar. 12, 2020; accepted in principle May 3, 2020; accepted for publication Jun. 11, 2020

Abstract A variety of shell colors are one of the most fundamental characteristics of molluscs, which have importantly ecological and economic significance. The Pacific oyster *Crassostrea gigas* is distributed in many sea areas around the world and also an aquacultured mollusc with high nutritional value. In this study, the whole soft body and the mantle tissue of black-shelled Pacific oyster (BSO) and white-shelled Pacific oyster (WSO) with starkly different melanin contents were compared, and the differences in physiology and metabolism between BSO and WSO were analyzed. The results of physiological indicators suggested BSO show more melanin, more dry matter, more crude lipid content, and stronger ability to scavenge free radicals than WSO. The altered metabolites of glycerophospholipids, fatty acyls, and steroids revealed different regulatory mechanisms of lipids. The correlation analysis of metabolomics and previously published RNAseq data suggested that BSO and WSO mainly differed in the basal metabolic processes, such as lipid, amino acid and purine metabolisms. This study provides insights into the changes in the physiological indictors and the metabolites of oysters with varying melanin content.

Keyword: *Crassostrea gigas*; UPLC-MS metabolomics; physiological indicators; melanin; shell color

1 INTRODUCTION

Colorful shells make molluscs quite attractive, but many bivalves such as oysters cannot detect color or even lack eyes completely (Wolken, 1988; Speiser and Johnsen, 2008; Morris, 2012; Wu et al., 2015, 2018). The function of molluscan shell color in bivalves could provide protection against predators with greater visual acuity and color vision, including apostatic selection (Moment, 1962; Smith, 1975) or countershading (Thayer, 1971). In addition, the darker color shells may also help molluscs heat up more than lighter one (Mitton, 1977) and some shell pigments could have demonstrated antimicrobial properties (Moret and Moreau, 2012). Shell color may offer camouflaged protection to avoid being spotted by predators (Hansson, 2004).

Shell color polymorphism, a characteristic trait of the molluscs, is the one of the focal points of molluscan biodiversity conservation (Williams, 2017) and also a common phenotype of economically important molluscs (Liu et al., 2009). In nature, oysters are rich in shell color diversity and the Pacific oyster *Crassostrea gigas* has been bred to obtain characteristic varieties with black, white, and other shell colors (Feng et al., 2015). Previous studies have shown that the shell color of the molluscs is an important economic trait, which is controlled by the genetic factors and correlated to

* Supported by the Agricultural Variety Improvement Project of Shandong Province (No. 2019LZGC020), the National Natural Science Foundation of China (Nos. 41906088, 41876193, 31802328), the National Key R&D Program of China (No. 2018YFD0901400), the Special Funds for Taishan Scholars Project of Shandong Province, China (No. tsqn201812094), the Shandong Provincial Natural Science Foundation, China (No. ZR2019MC002), the Modern Agricultural Industry Technology System of Shandong Province, China (No. SDAIT-14-03), and the Plan of Excellent Youth Innovation Team of Colleges and universities in Shandong Province, China (No. 2019KJF004)
** Corresponding authors: lei819@126.com; wangxiaotong999@163.com

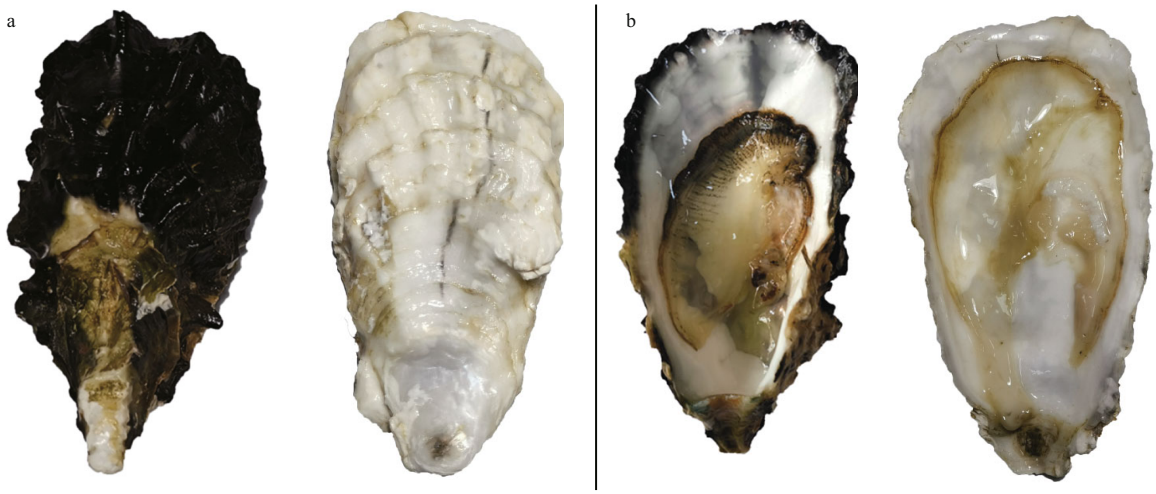

Fig.1 The appearance of the mantle and shell of Pacific oyster

a. the white and black shells; b. the white and black mantles.

multiple traits (Xu et al., 2017). The genetic basis of shell color has been well studied allowing the breeding of lines with specific colors. However, the effects of such pigmentation on molluscs have seldom been explored (Newkirk, 1980; Ding et al., 2015; Song et al., 2018).

Melanin is a biopolymer, which is one of the most widely distributed bio-pigments. It is generally black or brown, existing widely in the animals and plants. It is a biomacromolecule that is insoluble in water, acid or organic solvents (Lin and Fisher, 2007). Melanin can regulate a wide spectrum of molecular interactions and metabolic processes. It shows antioxidant and free radical scavenging activities and plays critical roles in the photoprotection and immune regulation (Videira et al., 2013; Chan et al., 2014). Therefore, melanin may serve broad applications in food processing, cosmetic development, and disease prevention and treatment (ElObeid et al., 2017).

The black-shelled Pacific oyster (BSO) and white-shelled Pacific oyster (WSO) are special varieties with black shell and white shell that the research team developed through 6 generations of individual selection. BSO shows greater melanin deposits in the shell and mantle tissue than that in WSO (Fig.1). Preliminary studies established a method to extract melanin from Pacific oysters, and showed that melanin pigmentation in Pacific oyster shells is significantly correlated with the melanin content in mantle tissues (Yu et al., 2017). A previous transcriptome data analysis showed that the mantle tissue of BSO with higher melanin content exhibited stronger antioxidant and free radical scavenging activities than that of WSO, and that these two oyster varieties might show different immune strategies (Wei et al., 2019). De novo assembly of BSO genome revealed that the divergence time was at about 2.2 million years ago between the BSO and the other *C. gigas* sequenced in 2012, which implied that species *C. gigas* had great intraspecific genetic variations (Zhang et al., 2012; Wang et al., 2019).

In order to understand the physiological and metabolic differences between BSO and WSO, in this study, we combined the fundamental biological characteristics between BSO and WSO with Ultra-High-Performance Liquid Chromatography-Mass Spectrometry (UPLC-MS) based metabolomics and correlation analysis with transcriptomics, and attempts to identify differences of these two oyster varieties in biochemical components, antioxidant activity, and metabolites. This comparative analysis between BSO and WSO may help to explain the ecological and physiological mechanism of mollusc pigmentation.

2 MATERIAL AND METHOD

2.1 Studied animal

Adult BSO and WSO (shell length: 8–10 cm) were sampled from a selectively bred population in Changdao, Yantai City of the Shandong Province in China. The sampled oysters were acclimated in filtered (1 μm) and aerated seawater (pH, 8.1; temperature, 18 °C; and salinity, 29) for 2 weeks before starting the experiment. During the acclimation period, the oysters were fed with *Isochrysis galbana*

at a concentration of 5.0×10^5 cells/mL three times daily. The seawater was renewed daily.

Each BSO and WSO group contained 75 oysters: 9 individuals from each group were randomly selected for dissection of the soft tissue for each of 6 indicators of biochemical components (dry matter, crude protein, crude lipid, ash, glycogen contents and fresh weight); another 9 individuals from each group were selected for the dissection of the mantles for pigmentation assay and antioxidant activities; for metabolomics analysis, the mantle tissues of the remaining 12 individuals from each group were used for the untargeted differential metabolite analysis. All tissues were flash frozen in liquid nitrogen and stored at -80 °C.

2.2 Measurement of biochemical components

The mantle edge pigmentation values (MPV) were measured as described previously, with some modifications (Debecker et al., 2015; Xing et al., 2018). The mantle edge (0.10 g) was dissected from each oyster and placed in a centrifuge tube containing 1 mL of 1.0 mol/L NaOH. The samples were then incubated in a water bath at 80 °C for 2 h and centrifuged at 12 000×*g* for 10 min. The supernatants were transferred to a spectrophotometer to analyze the total melanin content at 400 nm (A400). The A400 values were used to represent the total melanin content, and the absorbance values of the samples in the path-length cuvettes were read to three decimal places (Wei et al., 2019).

Dry matter, crude protein, crude lipid, ash, glycogen contents and fresh weight in the soft tissue of the two oyster varieties were determined using the direct drying method, Kjeldahl method, Soxhlet extraction method, muffler furnace high-temperature burning, and anthrone colorimetry, respectively (Berik et al., 2017; Hao et al., 2019).

2.3 Measurement of reducing power (RP), inhibition of linoleic acid oxidation (ILAO), and the scavenging activities of four free radicals

Six indices related to antioxidant activity, including RP, ILAO, and the scavenging activities of four free radicals [hydroxyl radical (HR), superoxide anion radical (SAR), 2,2-diphenyl-1-picrylhydrazyl (DPPH) radical, and 2,2'-azino-bis(3-ethylbenzothiazoline-6-sulfonic acid) (ABTS) radical] were measured in the mantle tissues of the two oyster varieties (Hu et al., 2017). The details of measurement of antioxidant activity are described in the Supporting Information.

2.4 UPLC-MS-based untargeted metabolomics

2.4.1 Sample

30-mg mantle tissue sample was weighed before transferred to a 1.5-mL tube containing small steel balls. Then, 20 μL each of 2-chloro-l-phenylalanine (0.3 mg/mL) and C-17 (0.01 mg/mL) dissolved in methanol as the internal standard, and 400 μL mixture of methanol and water (4/1, v/v) were added and the tubes were placed at -80 °C for 2 min. This was followed by grinding at 60 Hz for 2 min, ultrasonication in iced water for 10 min after vortexing, and freezing at -20 °C for 20 min. The samples were then centrifuged at 20 000×*g* for 10 min, 4 °C. The supernatants (200 μL) were collected and transferred to the vials after filtered by 0.22-μm microfilters. All the samples were stored at -80 °C until LC-MS analysis.

2.4.2 UPLC-MS

The metabolic profiles in both positive and negative ion modes was identified by ACQUITY UPLC system (Waters Corporation, Milford, USA) coupled with AB SCIEX Triple TOF 5600 System (AB SCIEX, Framingham, MA) and ACQUITY UPLC BEH C18 column (1.7 mm×2.1 mm×100 mm). The binary gradient elution system of the separation was composed of acetonitrile (containing 0.1% formic acid, v/v) and water (containing 0.1% formic acid, v/v). The injection volume was 5 μL. The flow rate was 0.4 mL/min, and the column temperature was 45 °C. The injection volume, flow rate and column temperature were set to 5 μL, 0.4 mL/min, and 45 °C respectively. The full scan mode (*m*/*z*, 70–1 000) combined with the Information Dependent Acquisition (IDA) mode was used for data acquisition. The parameters of mass spectrometry were as follows: ion source temperature, 550 °C (+) and 550 °C (−); ion spray voltage, 5 500 V (+) and 4 500 V (−); curtain gas of 35 psi; de-clustering potential, 100 V (+) and -100 V (−); collision energy, 10 eV (+) and -10 eV (−); and interface heater temperature, 550 °C (+) and 600 °C (−). For IDA analysis, the m/z range was set at 50–1 000 and the collision energy was 30 eV. In order to assess the repeatability of the data, Quality control (QC) samples were used every 10 samples at regular intervals in the process of analytical run (Zhu et al., 2019; Yin et al., 2020).

2.4.3 Data pre-processing and statistical analysis

The raw UPLC-MS data were identified by Progenesis QI v2.3 (Nonlinear Dynamics, Newcastle, UK) using the following parameters: precursor

Table 1 Biochemical components between BSO and WSO

Biochemical component	WSO	BSO
Mantle edge pigmentation	1.48±0.15	2.56±0.14**
Dry matter content (%)	12.72±2.53	16.86±1.70**
Crude lipid (%)	0.95±0.40	1.69±0.20**
Crude protein (%)	12.72±1.52	12.45±0.90
Ash (%)	2.77±0.17	2.68±0.10
Glycogen content (%)	2.27±0.28	2.18±0.28
Fresh weight (g)	18.26±3.96	18.83±4.96

**: $P<0.01$. In mean±SD; $n=9$.

tolerance, 5×10^{-6}; product tolerance, 10×10^{-6}; and product ion threshold, 5%. The qualitative compounds were screened according to the score. The screening threshold was a score of 30 (out of 60), and any score below 30 was deemed inaccurate and was deleted. The positive and negative data were combined and analyzed by SIMCA software (version 14.0, Umetrics, Umeå, Sweden). The alterations of metabolites between BSO and WSO were visualized by the principal component analysis (PCA) and (orthogonal) partial least-squares-discriminant analysis (OPLS-DA). The default 7-round cross-validation and 200 response permutation testing were applied to verify the quality of the models in order to guard against over-fitting.

In the OPLS-DA model analysis, total contribution of each variable was determined by the variable importance in the projection (VIP), the group discrimination was considered chiefly by the variables with VIP>1.

2.4.4 Identification of differential metabolites

A statistically significant threshold of VIP values (VIP>1.0) and P values ($P<0.05$) were selected to tell the differential metabolites. The metabolites were identified by Progenesis QI (Waters Corporation, Milford, USA) based on the public databases including the Human Metabolome Database (HMDB), Lipidmaps (v2.3), and METLIN.

2.5 Analysis of correlation between metabolomics and transcriptomics data

Previously published transcriptomics data showed a total of 1 288 genes was identified as differentially expressed genes (DEGs) in mantles by comparing WSO and BSO ($P<0.05$). The DEGs from BSO mantles had more genes upregulated compared with WSO mantles, 735 genes versus 553 genes, respectively (Wei et al., 2019). All pathway maps and relevant annotated information files of *C. gigas* were downloaded from the Kyoto Encyclopedia of Genes and Genomes (KEGG, http://www.genome.jp/kegg/) and collated to construct the KEGG background database for *C. gigas*. Then, the GeneID of the differentially expressed genes and EntryID of the differentially expressed metabolites between BSO and WSO were used, respectively, to search the relevant information in the collated database (Kanehisa et al., 2008). If at least one differential gene and one differential metabolite coexisted in a certain pathway, they were selected. Subsequently, each of the previously searched differential genes and metabolites were integrated into related metabolic pathways.

3 RESULT

3.1 Comparison of biochemical components and antioxidant activity

The contents of MPV in the mantle tissue and basic nutrients in the whole body of BSO and WSO are listed in Table 1. The melanin content of BSO was 1.8 times higher than WSO. The melanin content in the mantle tissue was significantly different between the two oysters ($P<0.01$), reflecting striking fundamental differences in their shell color phenotypes (Wei et al., 2019). The dry matter and crude lipid content of BSO was 1.3 times and 1.7 times higher than that of WSO, respectively. However, there were no significant differences observed in the crude protein, ash, and glycogen contents or fresh weight.

The antioxidant activities of the mantle tissue of BSO and WSO are presented in Fig.2. The RP and ILAO levels of BSO were significantly higher than those of WSO ($P<0.05$), and the SAR ($P<0.05$) and DPPH ($P<0.01$) scavenging activities of BSO were significantly higher than those of WSO. However, there was no significant difference in HR and ABTS scavenging activities between BSO and WSO.

3.2 Comparative metabolomics

The untargeted metabolomic profiling was performed on both the BSO and WSO mantle tissues, and the data were separately captured at the positive and negative ion modes. A total of 1 801 and 1 182 metabolite ion features were detected in the positive and negative ion modes, respectively. Since two datasets were obtained from the same set of samples, subsequent statistical analyses were performed in the same ion mode for model construction.

To evaluate the differential metabolic profiles

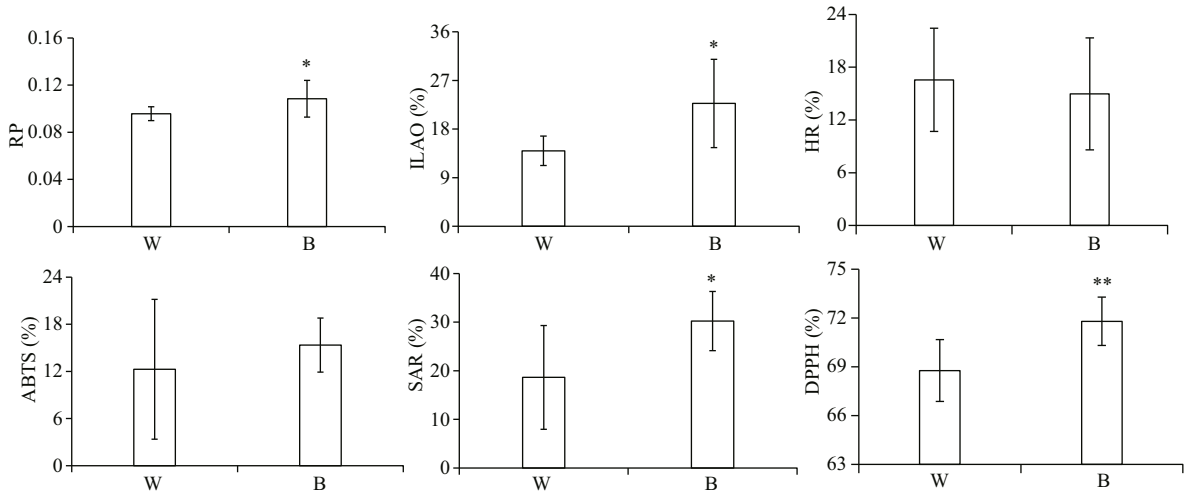

Fig.2 Antioxidant activities between BSO and WSO

* $P<0.05$; ** $P<0.01$. B and W represent BSO and WSO respectively. RP: reducing power; ILAO: inhibition of linoleic acid oxidation; HR: scavenging activity of hydroxyl radical; ABTS: scavenging activity of ABTS radical; SAR: scavenging activity of superoxide anions radical; DPPH: scavenging activity of DPPH radical.

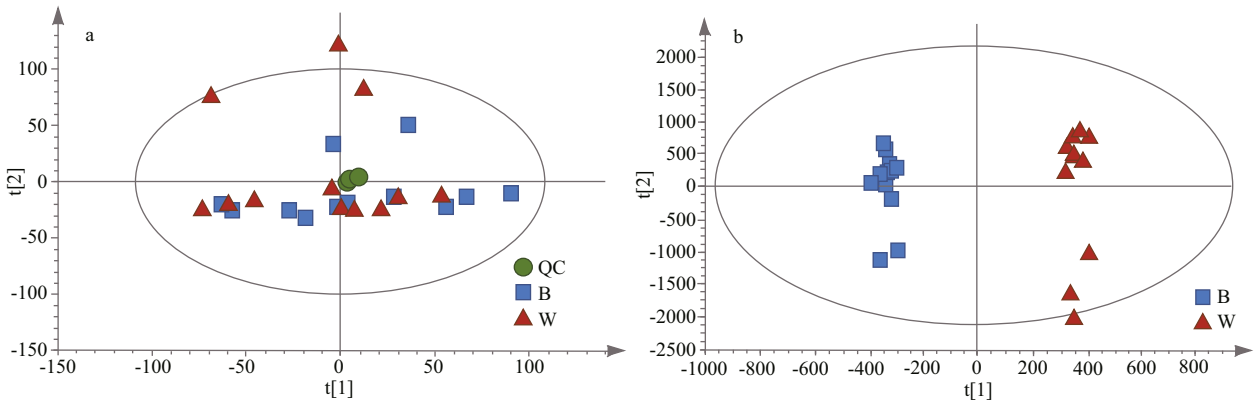

Fig.3 PCA score plots with QC samples (a), OPLS-DA score plots (b)

B and W represent BSO and WSO, respectively.

between BSO and WSO, unsupervised PCA was employed, which revealed that the QC samples were closely clustered together, indicating that the experiment was stable and reproducible. Figure 3a shows the first and second principal components, together explaining 34.75% of variance (18.90% and 15.85%, respectively). BSO and WSO were accurately classified and identified based on the metabolic profiles.

Furthermore, to distinguish the major metabolites between BSO and WSO, supervised OPLS-DA was performed to obtain better sample separation. The OPLS-DA score plot showed that BSO and WSO were clearly separated (Fig.3b). The values of R2X, R2Y, and Q2 of cross-validation in the OPLS-DA score plot were found to be 0.779, 0.994, and 0.838, respectively, indicating the model could precisely explain the sample differences and assess the model fitting over 200 iterations without over-fitting. A total of 141 metabolites were filtered out in the positive and negative ion modes (98 and 43, respectively). As compared with WSO, 72 were downregulated and 69 were upregulated in BSO (Supplementary Fig.S1). These metabolites could be classified into 6 main categories: glycerophospholipids, fatty acyls, amino acids, steroids, others, and unclassified (Supplementary Table S1). Glycerophospholipids formed majority of the functional category, accounting for at least 35% of differential metabolites in the mantle tissue. The differential metabolomic pathways that occur in the mantle tissue between BSO and WSO are summarized in Fig.4, according to the KEGG pathway analysis.

3.3 Correlation analysis of metabolomics and transcriptomics

In this study, metabolomic and previously published transcriptomic data were combined for a correlation analysis between BSO and WSO (Wei et al., 2019). A total of 13 KEGG pathways were

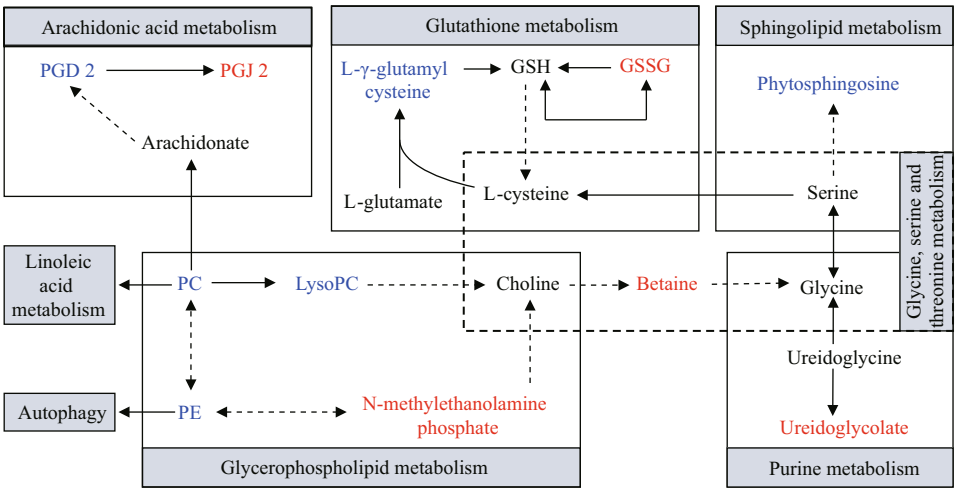

Fig.4 Hypothesized scheme of the metabolism pathways in mantles between BSO and WSO

Compared with WSO, the metabolites colored with red and blue indicate the up- and down-regulated metabolites in BSO, respectively. PGD2: prostaglandin D2; PGJ2: prostaglandin J2; GSH: glutathione; GSSG: oxidized glutathione; PC: phosphatidylcholine (14:0/16:1(9Z)); LysoPC: lysophosphatidylcholine (15:0); PE: phosphatidylethanolamine (18:3(9Z,12Z,15Z)/24:0).

associated with differentially expressed genes and metabolites (Supplementary Table S2). A total of 44 genes were associated with 14 metabolites (Supplementary Tables S3 & S4). The related genes and metabolites were mainly involved in the lipid, amino acid, and purine metabolic pathways, neuroactive ligand-receptor interactions, ABC transporters and autophagy-animal. The basal metabolic processes of the lipid, amino acid, and purine metabolisms, which were enriched by the correlation analysis between BSO and WSO, are summarized in Fig.5. The lipid metabolism mainly involves the metabolism of glycerophospholipid, arachidonic acid, linoleic acid, and α-linolenic acid. The amino acid metabolism mainly involves the metabolism of glycine, serine, threonine, histidine, tyrosine, tryptophan, and glutathione.

4 DISCUSSION

4.1 More melanin, more dry matter, more crude lipid content and stronger ability to scavenge free radicals in BSO

The detection of the basic nutrient indicators revealed that the contents of some nutrients in the whole body of oysters were similar. Based on these results, both oyster varieties can constitute low-fat, nutritious, and easily digestible food regardless of their shell color and are thus more suited to consumer requirement for a healthy diet, as compared to other meat foods (Gebhardt and Thomas, 2002). However, dry matter and crude lipid contents of BSO were significantly higher than those of WSO (P<0.01), suggesting that the potential commodity value of BSO. Although the crude lipid content of BSO was significantly higher than that of WSO, it remained much lower than that of the fish and terrestrial animals (Asha et al., 2014).

The homogenates from the soft tissues of the oysters are good antioxidants that can scavenge free radicals in vivo, thus, achieving antioxidant, and anti-aging health effects (Dong et al., 2010). Moreover, melanin can play antioxidant functions. Our results also demonstrate that the mantle tissue of the two oyster varieties may show strong antioxidant activities, with BSO showing significantly stronger ability to scavenge free radicals, specifically the SAR and DPPH scavenging activities, than WSO.

The free radicals are atoms or groups with unpaired electrons, such as DPPH ($DPPH^{\cdot}$), hydroxyl ($OH^{\cdot}$) or superoxide ($O_2^{\cdot-}$) radicals formed under photothermal conditions (McCord, 1985). The free radicals are harmful compounds produced during the biochemical oxidative reactions, with strong oxidative potential that can damage the tissues and cells of the organism, thus, causing chronic diseases, and aging (Green et al., 2009). The melanin of BSO may play a protective role under photothermal conditions to enhance its environmental adaptability.

4.2 The alteration of lipid metabolism between BSO and WSO

In this study, comparative metabolomic analysis based UPLC-MS revealed a total of 49/141 differentially expressed glycerophospholipids between BSO and WSO, and more

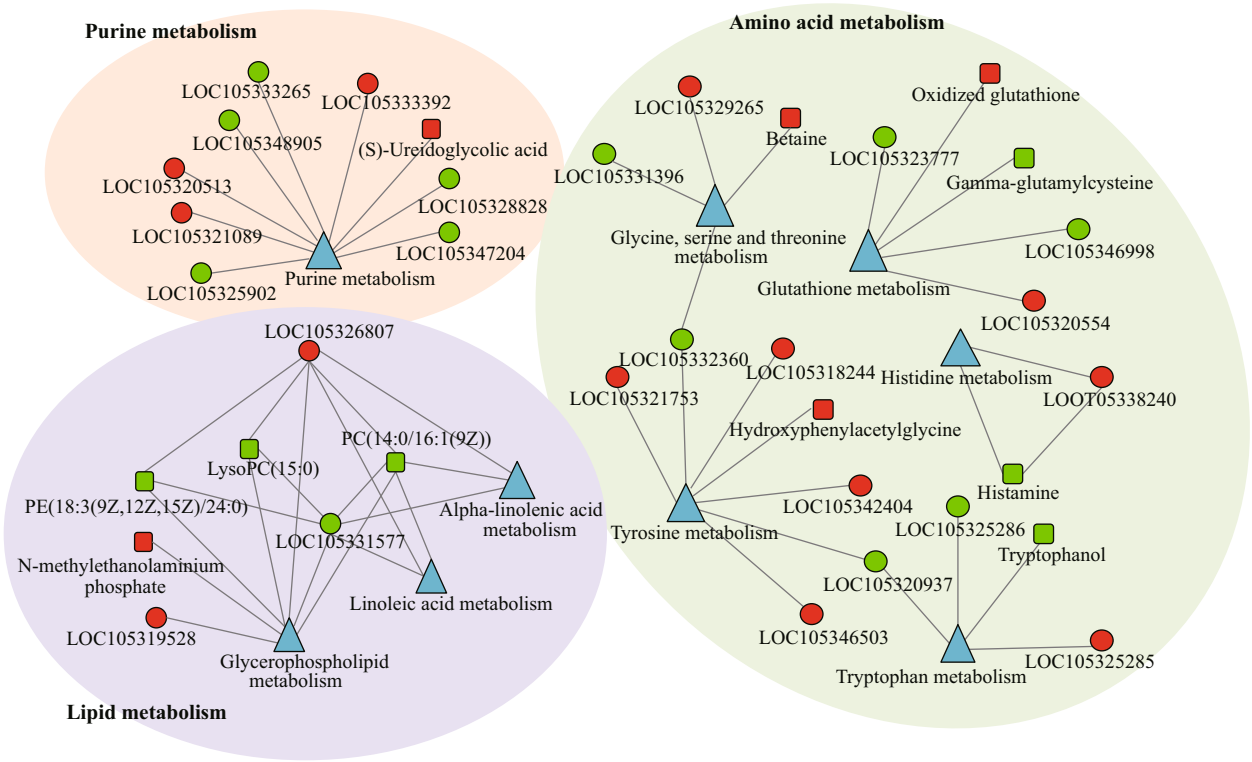

Fig.5 The basal metabolic processes which were enriched by the correlation analysis between BSO and WSO

Rectangle indicates the metabolite; circle indicates the gene; triangle indicates the pathway. The genes and metabolites colored in red and green indicate the up- and down-regulated levels, respectively.

glycerophospholipids, sterols, and sphingolipids were found in BSO, which further indicated the differences in the lipid content between the two oyster varieties. These results suggest that there are certain differences in the structure and composition of the membrane lipids between BSO and WSO, which may lead to different regulatory mechanisms for many biological processes.

In bivalves, lipid is an essential component to maintain the normal functioning of the cells, tissues, and organs (Chen et al., 2017). Moreover, glycerophospholipids and sterols play structural roles in the membranes and regulatory roles similar to the other membrane lipids (Mochel, 2018). The composition and alteration of metabolites between BSO and WSO suggest that there are certain differences in the cell membrane lipids, such as glycerophospholipids, sterols, and sphingolipids, which may lead to different regulatory mechanisms for a wide spectrum of biological functions, such as activating cells, maintaining the balance of metabolism and hormone secretion, and enhancing immunity (Cullis and De Kruijff, 1979).

Most differential metabolites were found to be glycerophospholipids, specifically phospholipids with sn-2 as DHA or EPA chain. Among these, PC [14:0/16:1(9Z)], lysoPC (15:0), and PE [18:3(9Z,12Z,15Z)/24:0] were enriched in glycerophospholipid metabolism, as evidenced by KEGG analysis between BSO and WSO. PC and PE play important roles in the neurotransmission and membrane function, and lysoPC is presumably a transient intermediate of PC that activates several second messengers and plays an important role in biological signal transduction and can be used as an extracellular mediator of nervous system and intracellular signal transduction (Koizumi et al., 2010; Shen et al., 2012). The down regulated PC [14:0/16:1(9Z)] and PE [18:3(9Z,12Z,15Z)/24:0] were involved in the pathway of “linoleic acid metabolism” and “autophagy - animal”. Histamine is a rhodopsin-like amine, and prostaglandin D2 (PGD2) is a prostanoid, and both histamine and PGD2 are G protein-coupled receptors (GPCRs) (Jongejan and Leurs, 2005; Sedej et al., 2008). The down regulated histamine and PGD2-d4 were participates in the neuroactive ligand-receptor interaction.

4.3 Correlation analysis of metabolomics and transcriptomics

The correlation analysis of differentially expressed genes and metabolites between BSO and WSO further

illustrated the pathways of ABC transporters and autophagy were enriched.

Betaine and maltotriose are both carried by ABC transporters. However, betaine can be carried by mineral and organic ion transporters and maltotriose by oligosaccharide, polyol, and lipid transporters (Pierce et al., 1995; Dietvorst et al., 2005). The downregulated levels of maltotriose may suggest suppressed macromolecule transport, such as that of the lipids, and the upregulated betaine levels suggest enhanced inorganic small-molecule transport in BSO.

In addition, other comparative analysis of different shell colored oysters suggested the processes of calcium regulation and endocytosis might affect melanogenesis in the mantle of the oyster (Feng et al., 2015; Xu et al., 2019), and the mechanisms of melanosome transport had been proposed a decade ago (Van Den Bossche et al., 2006). Two of these models proposed that melanocores were internalized by the keratinocytes through phagocytosis, thus, the alteration of autophagy between BSO and WSO may related to the active processes of melanogenesis and melanin transport in BSO.

The deposition of pigments differs greatly between BSO and WSO. The complicated synthesis and deposition of melanin are regulated in many ways. Melanin has many physiological functions such as photoprotection, anti-oxidation, antimicrobial property and camouflage (Sharma et al., 2002). The secretory stratum corneum of the mantle of BSO is characterized by obvious melanin deposition. This study illustrates how the physiological processes of BSO are different from those of WSO from the perspective of metabolites. However, unfortunately, no metabolites related to deposition of melanin were directly identified due to the limitations of metabolite database. Differential metabolites do not have associated with pigmentation may be caused by the imperfect functional annotations of genes or metabolites (Eom et al., 2012). Therefore, the differences between the two varieties of oysters are not necessarily caused by deposition of melanin, and may be related to some other conditions like growth potential and timing of gametogenesis.

5 CONCLUSION

In conclusion, the results indicate the survival advantage and commodity value of BSO. The different metabolites of glycerophospholipids, fatty acyls, and steroids between BSO and WSO revealed different regulatory mechanisms of lipids by comparative metabolomics analysis. The correlation analysis of the metabolomics and transcriptomics suggested the different of the basal metabolic processes, such as lipid, amino acid, and purine metabolisms.

6 DATA AVAILABILITY STATEMENT

The MS raw data that support the findings of this study are available in figshare with the identifier. Dataset, https://doi.org/10.6084/m9.figshare.12261065.v1.

References

Asha K K, Anandan R, Mathew S, Lakshmanan P T. 2014. Biochemical profile of oyster *Crassostrea madrasensis* and its nutritional attributes. *The Egyptian Journal of Aquatic Research*, **40**(1): 35-41.

Berik N, Çankırılıgil E C, Gül G. 2017. Mineral content of smooth scallop (*Flexopecten glaber*) caught Canakkale, Turkey and evaluation in terms of food safety. *Journal of Trace Elements in Medicine and Biology*, **42**: 97-102.

Chan C F, Huang C C, Lee M Y, Lin Y S. 2014. Fermented broth in tyrosinase- and melanogenesis inhibition. *Molecules*, **19**(9): 13 122-13 135.

Chen Q S, Wang X C, Cong P X, Liu Y J, Wang Y M, Xu J, Xue C H. 2017. Mechanism of phospholipid hydrolysis for oyster *Crassostrea plicatula* phospholipids during storage using shotgun lipidomics. *Lipids*, **52**(12): 1 045-1 058.

Cullis P T, De Kruijff B. 1979. Lipid polymorphism and the functional roles of lipids in biological membranes. *Biochimica et Biophysica Acta* (*BBA*)-*Reviews on Biomembranes*, **559**(4): 399-420.

Debecker S, Sommaruga R, Maes T, Stoks R. 2015. Larval UV exposure impairs adult immune function through a trade-off with larval investment in cuticular melanin. *Functional Ecology*, **29**(10): 1 292-1 299.

Dietvorst J, Londesborough J, Steensma H Y. 2005. Maltotriose utilization in lager yeast strains: *MTT1* encodes a maltotriose transporter. *Yeast*, **22**(10): 775-788.

Ding J, Zhao L, Chang Y Q, Zhao W M, Du Z L, Hao Z L. 2015. Transcriptome sequencing and characterization of japanese scallop *Patinopecten yessoensis* from different shell color lines. *PLoS One*, **10**(2): e0116406.

Dong X P, Zhu B W, Zhao H X, Zhou D Y, Wu H T, Yang J F, Li D M, Murata Y. 2010. Preparation and *in vitro* antioxidant activity of enzymatic hydrolysates from oyster (*Crassostrea talienwhannensis*) meat. *International Journal of Food Science & Technology*, **45**(5): 978-984.

ElObeid A S, Kamal-Eldin A, Abdelhalim M A K, Haseeb A M. 2017. Pharmacological properties of melanin and its function in health. *Basic & Clinical Pharmacology & Toxicology*, **120**(6): 515-522.

Eom D S, Inoue S, Patterson L B, Gordon T N, Slingwine R, Kondo S, Watanabe M, Parichy D M. 2012. Melanophore

migration and survival during zebrafish adult pigment stripe development require the immunoglobulin superfamily adhesion molecule Igsf11. *PLoS Genetics*, **8**(8): e1002899.

Feng D D, Li Q, Yu H, Zhao X L, Kong L F. 2015. Comparative transcriptome analysis of the Pacific Oyster *Crassostrea gigas* characterized by shell colors: identification of genetic bases potentially involved in pigmentation. *PLoS One*, **10**(12): e0145257.

Gebhardt S E, Thomas R G. 2002. Nutritive Value of Foods. United States Department of Agriculture. Agricultural Research Service, Home and Garden Bulletin, Beltsville, Maryland.

Green T J, Dixon T J, Devic E, Adlard R D, Barnes A C. 2009. Differential expression of genes encoding anti-oxidant enzymes in Sydney rock oysters, *Saccostrea glomerata* (Gould) selected for disease resistance. *Fish & Shellfish Immunology*, **26**(5): 799-810.

Hansson L A. 2004. Plasticity in pigmentation induced by conflicting threats from predation and UV radiation. *Ecology*, **85**(4): 1 005-1 016.

Hao R J, Du X D, Yang C Y, Deng Y W, Zheng Z, Wang Q H. 2019. Integrated application of transcriptomics and metabolomics provides insights into unsynchronized growth in pearl oyster *Pinctada fucata martensii*. *Science of the Total Environment*, **666**: 46-56.

Hu S J, Zhao G H, Zheng Y X, Qu M, Jin Q, Tong C Q, Li W. 2017. Effect of drying procedures on the physicochemical properties and antioxidant activities of polysaccharides from *Crassostrea gigas*. *PLoS One*, **12**(11): e0188536.

Jongejan A, Leurs R. 2005. Delineation of receptor-ligand interactions at the human histamine H_1 receptor by a combined approach of site-directed mutagenesis and computational techniques - or - how to bind the H_1 receptor. *Archiv Der Pharmazie*, **338**(5-6): 248-259.

Kanehisa M, Araki M, Goto S, Hattori M, Hirakawa M, Itoh M, Katayama T, Kawashima S, Okuda S, Tokimatsu T, Yamanishi Y. 2008. KEGG for linking genomes to life and the environment. *Nucleic Acids Research*, **36**(S1): D480-D484.

Koizumi S, Yamamoto S, Hayasaka T, Konishi Y, Yamaguchi-Okada M, Goto-Inoue N, Sugiura Y, Setou M, Namba H. 2010. Imaging mass spectrometry revealed the production of lyso-phosphatidylcholine in the injured ischemic Rat Brain. *Neuroscience*, **168**(1): 219-225.

Lin J Y, Fisher D E. 2007. Melanocyte biology and skin pigmentation. *Nature*, **445**(7130): 843-850.

Liu X, Wu F C, Zhao H E, Zhang G F, Guo X M. 2009. A novel shell color variant of the pacific abalone *Haliotis discus hannai* Ino subject to genetic control and dietary influence. *Journal of Shellfish Research*, **28**(2): 419-424.

McCord J. 1985. Oxygen-derived free radicals in postischemic tissue injury. *New England Journal of Medicine*, **312**(3): 159-163.

Mitton J B. 1977. Shell color and pattern variation in *Mytilus edulis* and its adaptive significance. *Chesapeake Science*, **18**: 387-390.

Mochel F. 2018. Lipids and synaptic functions. *Journal of Inherited Metabolic Disease*, **41**(6): 1 117-1 122.

Moment G B. 1962. Reflexive selection: a possible answer to an old puzzle. *Science*, **136**(3512): 262-263.

Moret Y, Moreau J. 2012. The immune role of the arthropod exoskeleton. *Invertebrate Survival Journal*, **9**: 200-206.

Morris P. 2012. Animal eyes (Oxford Animal Biology Series) by Michael F. Land & Dan-Eric Nilsson. *Zoological Journal of the Linnean Society*, **166**(4): 912.

Newkirk G F. 1980. Genetics of shell color in *Mytilus edulis* L. and the association of growth rate with shell color. *Journal of Experimental Marine Biology and Ecology*, **47**(1): 89-94.

Pierce S K, Rowland-Faux L M, Crombie B N. 1995. The mechanism of glycine betaine regulation in response to hyperosmotic stress in oyster mitochondria: a comparative study of Atlantic and Chesapeake Bay oysters. *Journal of Experimental Zoology*, **271**(3): 161-170.

Sedej M, Platzer W, Vukoja A, Schuligoi R, Peskar B A, Heinemann Á, Waldhoer M. 2008. Effects of PGH_2 and PGD_2 on CRTH2 and DP receptors in primary cells and co-expressed in HEK293 cells. *BMC Pharmacology*, **8**(S1**)**: A10.

Sharma S, Wagh S, Govindarajan R. 2002. Melanosomal proteins—role in melanin polymerization. *Pigment Cell Research*, **15**(2): 127-133.

Shen Q, Wang Y Y, Gong L K, Guo R, Dong W, Cheung H Y. 2012. Shotgun lipidomics strategy for fast analysis of phospholipids in fisheries waste and its potential in species differentiation. *Journal of Agricultural and Food Chemistry*, **60**(37): 9 384-9 393.

Smith D A S. 1975. Polymorphism and selective predation in *Donax faba* Gmelin (Bivalvia: Tellinacea). *Journal of Experimental Marine Biology and Ecology*, **17**(2): 205-219.

Song J L, Li Q, Yu Y, Wan S, Han L C, Du S J. 2018. Mapping genetic loci for quantitative traits of golden shell color, mineral element contents, and growth-related traits in Pacific Oyster (*Crassostrea gigas*). *Marine Biotechnology*, **20**(5): 666-675.

Speiser D I, Johnsen S. 2008. Comparative morphology of the concave mirror eyes of scallops (Pectinoidea). *American Malacological Bulletin*, **26**(1-2): 27-33.

Thayer C W. 1971. Fish-like crypsis in swimming monomyaria. *Journal of Molluscan Studies*, **39**(5): 371-376.

Van Den Bossche K, Naeyaert J M, Lambert J. 2006. The quest for the mechanism of melanin transfer. *Traffic*, **7**(7): 769-778.

Videira I F D S, Moura D F L, Magina S. 2013. Mechanisms regulating melanogenesis. *Anais Brasileiros de Dermatologia*, **88**(1): 76-83.

Wang X T, Xu W J, Wei L, Zhu C L, He C, Song H C, Cai Z Q, Yu W C, Jiang Q Y, Li L L, Wang K, Feng C G. 2019. Nanopore sequencing and *de novo* assembly of a black-shelled Pacific oyster (*Crassostrea gigas*) genome. *Frontiers in Genetics*, **10**: 1 211.

Wei L, Jiang Q Y, Cai Z Q, Yu W C, He C, Guo W, Wang X T.

2019. Immune-related molecular and physiological differences between black-shelled and white-shelled Pacific oysters *Crassostrea gigas*. *Fish & Shellfish Immunology*, **92**: 64-71.

Williams S T. 2017. Molluscan shell colour. *Biological Reviews*, **92**(2): 1 039-1 058.

Wolken J J. 1988. Photobehavior of marine invertebrates: extraocular photoreception. *Comparative Biochemistry and Physiology Part C*: *Comparative Pharmacology*, **91**(1): 145-149.

Wu C L, Jiang Q Y, Wei L, Cai Z Q, Chen J, Yu W C, He C, Wang J, Guo W, Wang X T. 2018. A rhodopsin-like gene may be associated with the light-sensitivity of adult pacific oyster *Crassostrea gigas*. *Frontiers in physiology*, **9**: 221.

Wu C L, Wang J, Yang Y J, Li Z, Guo T, Li Y C, Wang X T. 2015. Adult pacific oyster (*Crassostrea gigas*) may have light sensitivity. *PLoS One*, **10**(10): e0140149.

Xing D, Li Q, Kong L F, Yu H. 2018. Heritability estimate for mantle edge pigmentation and correlation with shell pigmentation in the white-shell strain of Pacific oyster, *Crassostrea gigas*. *Aquaculture*, **482**: 73-77.

Xu L, Li Q, Yu H, Kong L F. 2017. Estimates of heritability for growth and shell color traits and their genetic correlations in the black shell strain of Pacific Oyster *Crassostrea gigas*. *Marine Biotechnology*, **19**(5): 421-429.

Xu M, Huang J, Shi Y, Zhang H, He M X. 2019. Comparative transcriptomic and proteomic analysis of yellow shell and black shell pearl oysters, *Pinctada fucata martensii*. *BMC Genomics*, **20**(1): 469.

Yin P P, Jia A R, Heimann K, Zhang M S, Liu X, Zhang W, Liu C H. 2020. Hot water pretreatment-induced significant metabolite changes in the sea cucumber *Apostichopus japonicus*. *Food Chemistry*, **314**: 126211.

Yu W C, He C, Cai Z Q, Xu F, Wei L, Chen J, Jiang Q Y, Wei N, Li Z, Guo W, Wang X T. 2017. A preliminary study on the pattern, the physiological bases and the molecular mechanism of the adductor muscle scar pigmentation in Pacific oyster *Crassostrea gigas*. *Frontiers in Physiology*, **8**: 699.

Zhang G F, Fang X D, Guo X M, Li L, Luo R B, Xu F, Yang P C, Zhang L L, Wang X T, Qi H G, Xiong Z Q, Que H Y, Xie Y L, Holland P W H, Paps J, Zhu Y B, Wu F C, Chen Y X, Wang J F, Peng C F, Meng J, Yang L, Liu J, Wen B, Zhang N, Huang Z Y, Zhu Q H, Feng Y, Mount A, Hedgecock D, Xu Z, Liu Y J, Domazet-Lošo T, Du Y S, Sun X Q, Zhang S D, Liu B H, Cheng P Z, Jiang X T, Li J, Fan D D, Wang W, Fu W J, Wang T, Wang B, Zhang J B, Peng Z Y, Li Y X, Li N, Wang J P, Chen M S, He Y, Tan F J, Song X R, Zheng Q M, Huang R L, Yang H L, Du X D, Chen L, Yang M, Gaffney P M, Wang S, Luo L H, She Z C, Ming Y, Huang W, Zhang S, Huang B Y, Zhang Y, Qu T, Ni P X, Miao G Y, Wang J Y, Wang Q, Steinberg C E W, Wang H Y, Li N, Qian L M, Zhang G J, Li Y R, Yang H M, Liu X, Wang J, Yin Y, Wang J. 2012. The oyster genome reveals stress adaptation and complexity of shell formation. *Nature*, **490**(7418): 49-54.

Zhu W H, Yu H T, Wang Y, Chang Y, Wan J Y, Xu N, Wang J L, Liu W S. 2019. Integration of transcriptomics, proteomics and metabolomics data to reveal the biological mechanisms of abrin injury in human lung epithelial cells. *Toxicology Letters*, **312**: 1-10.

Electronic supplementary material

Supplementary material (Supplementary Fig.S1, Tables S1–S4, and Supporting Information) is available in the online version of this article at https://doi.org/10.1007/s00343-020-0117-3.